Available online at www.sciencedirect.com
SCIENCE DIRECT®
International Journal of Heat and Mass Transfer 47 (2004) 671–681
International Journal of HEAT and MASS TRANSFER
www.elsevier.com/locate/ijhmt

Experimental investigation on heat transfer and frictional characteristics of spirally corrugated tubes in turbulent flow at different Prandtl numbers

P.G. Vicente [a,*], A. García [b], A. Viedma [b]

[a] Departamento de Ingeniería de Sistemas Industriales, Universidad Miguel Hernández, Avenida del Ferrocarril s/n, 03202 Elche, Spain

[b] Departamento de Ingeniería Térmica y de Fluidos, Universidad Politécnica de Cartagena, Campus de la Muralla del Mar, 30202 Cartagena, Spain

Received 25 September 2002; received in revised form 6 August 2003

Abstract

Corrugated tubes have been experimentally studied in order to obtain their heat transfer and isothermal friction characteristics. The use of water and ethylene glycol as test fluids has allowed to cover a wide range of turbulent fluid flow conditions: Reynolds number from 2000 to 90 000 and Prandtl number from 2.5 to 100.

The paper presents a comprehensive experimental study on a family of 10 corrugated tubes which were manufactured by cold rolling. Artificial roughness is characterised by rib height h/d ranging from 0.02 to 0.06 and spiral pitch p/d from 0.6 to 1.2. The results show that a unique dimensionless parameter named severity index ($\phi = h^2/pd$) can be used to establish roughness influence on flow.

The large amount of experimental data has been correlated in order to obtain easy to use expressions for Fanning friction factors and Nusselt numbers as functions of flow and geometry dimensionless parameters. The real benefits which are offered by corrugated tubes have been assessed by calculating one of the performance evaluation criteria commonly used in the enhanced heat transfer literature. Finally an optimisation study shows the guidelines to choose which roughness geometry offers the best performance for specific flow conditions.

1. Introduction

Spirally corrugated tubes have become important in commercial applications for turbulent one-phase flow due to:

1. The pressure drop increment is generally compensated by the heat transfer augmentation.
2. The amount of tube material used in the tube manufacturing neither increases nor decreases.
3. Manufacturing process is easy and cheap.

Corrugation increases heat transfer coefficient in turbulent flow by mixing the flow in the boundary layer and also by increasing the turbulence level of the fluid flow. In addition, when smooth tubes are deformed, the wet perimeter is increased and the cross-area is reduced, leading to a hydraulic diameter reduction.

Corrugated tubes are sometimes chosen in the design of shell-and-tube industrial heat exchangers. The size of these heat exchangers can be reduced considerably by using corrugated tubes instead of smooth tubes. Alternatively, the objective of applying an augmentation technique could be to increase the heat duty of a heat exchanger with an area previously fixed.

Fig. 1 shows an sketch of a single-start corrugated tube, where p stands for helical pitch; h for height of the ridge; and α for helical angle. The tube roughness is

* Corresponding author.
E-mail address: pedro.vicente@umh.es (P.G. Vicente).

0017-9310/$ - see front matter © 2003 Elsevier Ltd. All rights reserved.
doi:10.1016/j.ijheatmasstransfer.2003.08.005

Nomenclature

A	heat transfer area, $\pi d l_h$ (m^2)
c_p	specific heat of the test fluid ($J\,kg^{-1}\,K^{-1}$)
d	envelope (maximum inside) diameter (m)
h	roughness height, Fig. 1 (m)
h^+	roughness Reynolds number $(h/d)Re\sqrt{f/2}$
h_o	outside heat transfer coefficient ($W\,m^{-2}\,K^{-1}$)
h_i	inside heat transfer coefficient ($W\,m^{-2}\,K^{-1}$)
I	intensity (A)
k	thermal conductivity ($W\,m^{-1}\,K^{-1}$)
l_p	length of test section between pressure taps (m)
l_h	length of the heat transfer section (m)
$\dot{m}$	mass flow rate of the test fluid ($kg\,s^{-1}$)
p	helical pitch, Fig. 1 (m)
ΔP	pressure drop across the test section ($N\,m^{-2}$)
P	pumping power (W)
Q	heat transfer rate (W)
q''	heat flux, $VI/\pi d l_h$ ($W\,m^{-2}$)
t	temperature (K)
t_{wi}	inside surface temperature of the wall (K)
t_{wo}	outside surface temperature of the wall (K)
V	voltage (V)
U	overall heat transfer coefficient ($W\,m^{-2}\,K^{-1}$)
v	average velocity of the fluid ($m\,s^{-1}$)

Dimensionless groups

f	Fanning friction factor, $\Delta P d/2\rho v^2 l_p$
$G(h^+, Pr)$	heat transfer roughness function
Nu	Nusselt number, $h_i d/k$
Pr	Prandtl number, $c_p\mu/k$
Re	Reynolds number, $\rho v d/\mu$
$R(h^+)$	momentum transfer roughness function
St	Stanton number, $Nu/RePr$

Greek symbols

α	helix angle (°)
μ	dynamic viscosity ($kg\,m^{-1}\,s^{-1}$)
ρ	fluid density ($kg\,m^{-3}$)

Subscripts

a	augmented tube (corrugated tube)
b	based on bulk temperature
in	tube inlet
o	equivalent smooth tube value
out	tube outlet
s	smooth tube
w	based on wall temperature (inside surface)

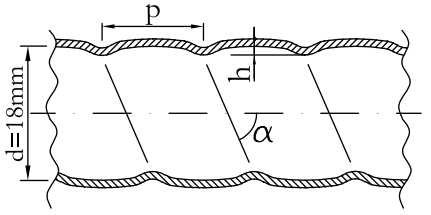

Fig. 1. Sketch of a single-start corrugated tube.

defined in non-dimensional form by the reduced height h/d and reduced pitch p/d. Additionally the severity index defined by $\phi = h^2/pd$ can be employed as the unique parameter to characterise the tube roughness.

Corrugated tubes have been widely studied during the last 30 years. Most of published experimental works focus on shell and tube condensers which are used in power plants [1]. In these surface condensers, water is the tube-side fluid and the typical flow conditions are: Prandtl numbers from 4 to 7 and Reynolds numbers from 10 000 to 90 000.

In order to reduce the scope of the study, eight experimental papers dealing with single-start corrugated tubes formed by cool rolling have been selected and carefully analysed. Other artificial roughness techniques such as spirally corrugation formed with internal mandrels, springs, transverse corrugation and transverse ribs, have not been considered. A summary of the experimental range covered by each of the analysed works is shown in Table 1. This includes: number of studied corrugated tubes, geometrical range and flow range analysed.

Most of the works listed in Table 1 were carried out employing water as the only test fluid. This leads to a reduced Prandtl number range, where heat transfer dependence on Prandtl number cannot be determined with a minimum level of accuracy. Moreover, since experiments were carried out using tubes with diameters from 16 to 30 mm, Reynolds number ranges are reduced as well. This leads to conclude that the flow behaviour inside corrugated tubes is not well known for typical viscous fluids conditions: high Prandtl numbers and low Reynolds numbers.

In order to compare experimental results from the different studies, the correlations proposed by each study have been solved for one tube of the following roughness: $h/d = 0.03$ and $p/d = 0.4$, at flow conditions $Pr = 6$ and $Re = 5000$–$100\,000$. Friction factor and heat transfer augmentations (f_a/f_s and Nu_a/Nu_s) are plotted in Figs. 2 and 3 respectively.

The graphical results show large disagreements among the correlations proposed by the different authors: at $Re = 10\,000$, friction factors augmentations between 1.3 and 3 and Nusselt number augmentations

Table 1
Experimental range covered by the studies published in the literature available [2–9]

Paper	N_{tub}	d [mm]	$h/d \times 10^3$	p/d [–]	$Re \times 10^3$	Pr
Mehta and Raja Rao [2]	11	15.9	8–88	0.20–0.78	10–80	4–6
Gupta and Raja Rao [3]	12	22.0–25.0	20–62	0.20–1.20	6–60	5.0
Withers [4]	14	13.9–29.9	16–52	0.30–0.91	10–120	5–10
Li et al. [5]	16	17.0–17.9	10–69	0.14–0.97	10–80	5–7
Ganeshan and Raja Rao [6]	4	25.4–25.7	21–30	1.17–1.18	10–100	4.3
Sethumadhavan and Raja Rao [7]	2	25.4–25.7	26–30	1.17–1.18	3–70	4.7–35
Zimparov et al. [8]	25	24.9–26.1	17–47	0.25–0.67	10–60	2.2–3.4
Ravigururajan and Bergles [9]	3	23.6	6–22	0.81	3–50	5.8–10

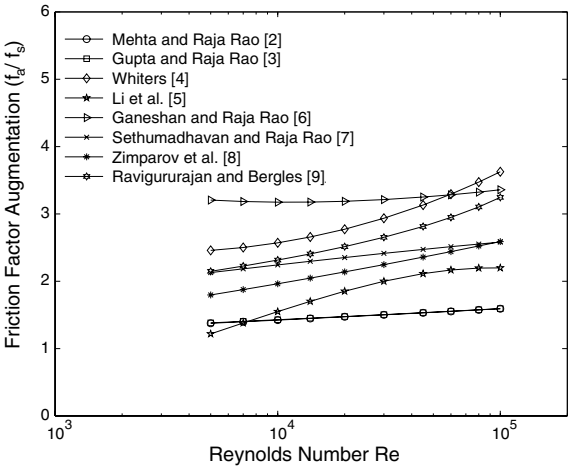

Fig. 2. Comparison among different correlations proposed to determine friction factor augmentation produced by a corrugated tube: $h/d = 0.03$ and $p/d = 0.4$.

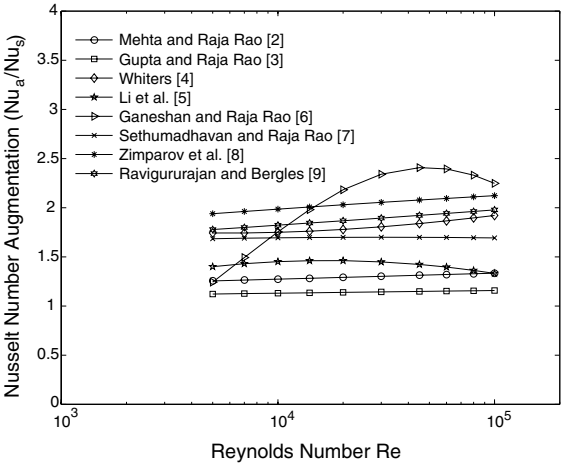

Fig. 3. Comparison among different correlations proposed to determine heat transfer augmentation produced by a corrugated tube: $h/d = 0.03$ and $p/d = 0.4$ (constant fluid properties and $Pr = 6$).

between 1.2 and 2 are observed. Rabas et al. [1] also compared different experimental works and concluded that there is a substantial scatter among the correlations; they did not find any obvious reason to select any of the proposed prediction methods.

From the above analysis it can be concluded that, although there is a great amount of experimental works on spirally corrugated tubes, more experimental data are required to: (1) obtain reliable correlations for heat transfer and pressure drop in a wider range of flow conditions, (2) clarify the large differences between correlations, (3) determine heat transfer dependence on Prandtl number, and (4) determine the optimum geometry depending on flow conditions.

The main aim of the present paper is to obtain experimental data to characterise the internal friction factor and Nusselt numbers in corrugated tubes in wide flow conditions. A large amount of new experimental data has been obtained for 10 corrugated tubes of different roughness geometry (h/d and p/d). The main contribution of this work is the wide range of flow conditions covered in terms of Re and Pr. This has allowed to establish the heat transfer dependence on Prandtl number. Finally, it has been established the optimum corrugation geometry as a function of Reynolds and Prandtl numbers.

2. Tested tubes

The experimental study was carried out on a family of 10 spirally corrugated tubes (commercially known as *hard tubes*). Tubes were manufactured from stainless steel plain tubes and had inner diameters of 18 mm and a wall thickness of 1 mm before the rolling operation took place. Corrugated tubes were manufactured by cold rolling the outer surface, which produces an internal spirally ridging similar to the external grooving.

Table 2 shows the geometrical parameters of the corrugated tubes which have been studied in this work.

Table 2
Corrugated tubes dimensions: maximum internal diameter d, corrugation height h, helical pitch p, dimensionless height h/d, dimensionless pitch p/d and severity index ϕ

Tube no.	d [mm]	h [mm]	p [mm]	h/d [–]	p/d [–]	$\phi \times 10^3$ [–]
01	18.0	1.03	15.95	0.0572	0.886	3.694
02	18.0	0.67	15.95	0.0372	0.886	1.563
03	18.0	0.43	15.86	0.0239	0.881	0.648
04	18.0	0.48	10.94	0.0267	0.608	1.170
05	18.0	0.67	12.90	0.0372	0.717	1.932
06	18.0	0.87	12.98	0.0483	0.721	3.239
07	18.0	0.91	18.27	0.0506	1.015	2.519
08	18.0	0.60	21.14	0.0333	1.174	0.946
09	18.0	0.92	22.11	0.0511	1.229	2.126
10	18.0	0.48	20.84	0.0267	1.158	0.614

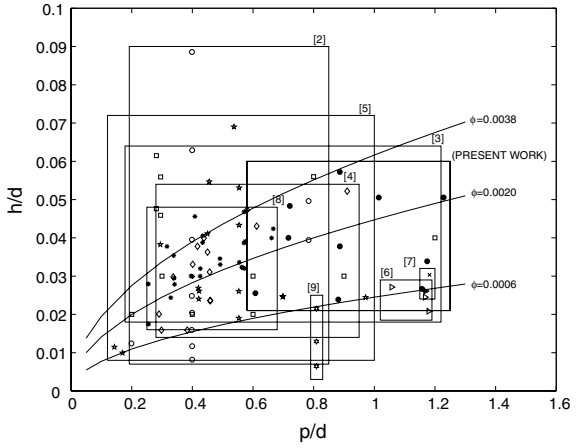

Fig. 4. Dimensionless height h/d vs. dimensionless pitch p/d. Present work geometrical range in comparison to other papers [2–9].

A comparison between the geometrical range studied at the present work and those from other experimental investigations is shown in Fig. 4.

The range of roughness geometry was as wide as allowed the capability of the manufacturing process, which depends on: (1) plain tube dimensions (diameter and wall thickness), (2) tube material, and (3) manufacturing capacity to deform. Corrugation depth (so-called corrugation height) depends on the distance between the tube wall and the corrugation wheel, whereas helical pitch depends on the angle formed by the wheel and the plain tube axis.

After the cold deformation process, it is considered that the maximum inner diameter is the original plain tube diameter, and it has been used as length scale for Re, Nu and f. This approach was recommended by Marner et al. [10], since it allows comparisons among the performance of the enhanced tubes from different manufacturers.

3. Experimental set-up

An schematic diagram of the experimental set-up is shown in Fig. 5. Pressure drop and heat transfer studies were carried out for the turbulent flow of water (at 30–65 °C) and ethylene glycol (at 30–55 °C) covering a continuous Reynolds range from 2000 to 90 000. The experimental set-up and procedure are described in a previous paper [11] and with further details in [12].

Heat transfer experiments were carried out under constant heat flux conditions, where energy is added to the working fluid by alternating current Joule heating. Pressure drop tests were carried out in the hydrodynamic developed region under isothermal conditions.

To keep a constant temperature in the tank, a cooling circuit was added. This secondary loop consisted of a variable-speed centrifugal pump, a double-pipe heat exchanger and an electrical heater. The fluid was cooled by chilled water in the counterflow heat exchanger. The electrical heater, controlled by a PID, allowed for adjusting the temperature in the tank to the desirable value.

Heat transfer tests were carried out at five different Prandtl numbers: 92, 59, 37, 4.2 and 2.9, working with ethylene glycol at 40, 55 and 70 °C and water at 40 and 60 °C. Fluid inlet and outlet temperatures t_{in}, t_{out} were measured by submerged type RTDs. Outer wall temperature was measured at one axial position by 12 surface type RTDs spaced 30°. The circumferential wall temperature at $x/d = 35$ was used to calculate the Nusselt number. At this location the flow is fully developed and the local Nusselt number is the asymptotic Nusselt number.

Nusselt number calculations were corrected by a factor $(\mu_b/\mu_w)^{-0.14}$ that considers the fluid viscosity variations at the boundary layer. The 0.14 exponent was used in Sieder–Tate equation and by Sethumadhavan and Raja Rao [7] and the results hardly varied with respect to the more widely used 0.11 exponent, proposed by Kays and London [13].

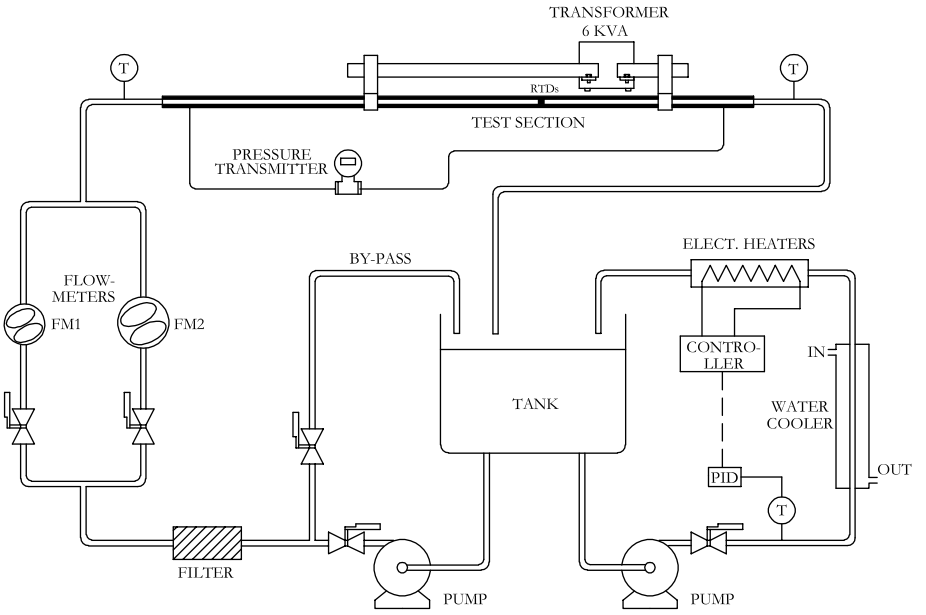

Fig. 5. A schematic diagram of the experimental set-up.

Isothermal pressure drop studies were done with water at 25 and 55 °C and ethylene glycol at 55 °C to cover a continuous Reynolds number range from 2000 to 90 000. Fanning friction coefficients were determined from fluid flow rate and pressure drop measurements. A highly accurate pressure transmitter was used to measure the pressure drop along a 5.2 m tube length.

Experimental uncertainty was calculated following Kline and McClintock [14] method based on a 95% confidence level. Instrumentation errors were as follows: temperature, 0.08 °C; flow rate, 0.4% full scale; differential pressure 0.075% span; intensity 0.1% measure + 0.04% full scale; and voltage, 0.04% measure + 0.03% full scale. To the thermophysical properties of the tested fluids have been assigned an uncertainty of ±0.5% to ρ and ±1% to μ, c_p and k. An uncertainty of 0.1% has been allocated to the inner diameter of the test tube. Test section length uncertainties were 5 mm for the pressure test section and 10 mm for the heat transfer test section.

Uncertainty calculations showed maximum values of 4% for Reynolds number, 3.5% for Prandtl number, 3% for friction factor and 4.5% for Nusselt number.

4. Results and discussion

4.1. Pressure drop

Isothermal pressure drop experiments were performed in one smooth and 10 corrugated tubes. Water and ethylene glycol were used as test fluids, and a Reynolds number range from 200 to 90 000 was covered. The present work focuses on turbulent flow. Therefore only results from transition to $Re = 90\,000$ are discussed, while laminar and transition results will appear in a future paper.

Pressure drop experiments with a smooth tube were carried out so as to adjust the experimental set-up and check its uncertainties. A maximum deviation of 3% with respect to the widely employed Blasius equation ($f_s = 0.079Re^{-0.25}$) was found. This deviation was in accordance with the uncertainty analysis, and assured a proper instrumentation adjustment.

Pressure drop experiments were carried-out in the 10 corrugated tubes described at Table 2. The results are shown as Fanning friction factor versus Reynolds number in Fig. 6. Around 60 experimental points for each tube were obtained. The use of water and ethylene glycol at different temperatures allowed to cover a continuous Reynolds number range.

The set of corrugated tubes are supposed to be geometrically similar. Through a non-dimensional analysis, it can be demonstrated that friction factor is a function of Reynolds number and roughness, characterised by two dimensionless numbers: dimensionless height h/d and dimensionless pitch p/d.

Friction factor experimental results from all test tubes (≈600 points) are correlated by the following equation:

$$f_a = 1.47(h/d)^{0.91}(p/d)^{-0.54}Re^{-0.16}. \quad (1)$$

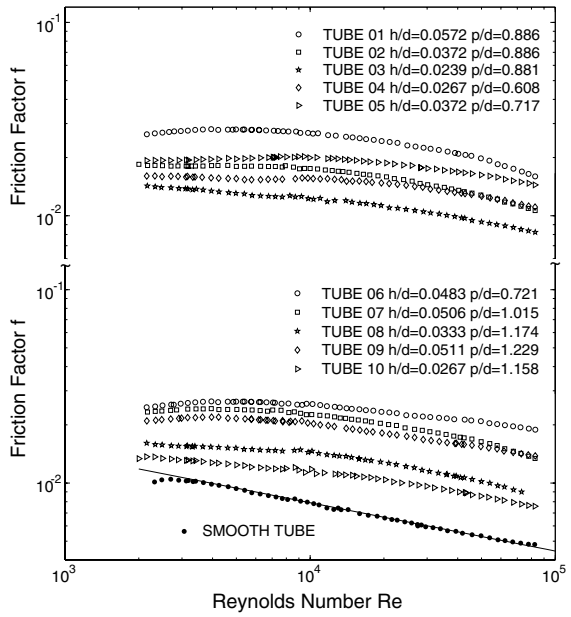

Fig. 6. Fanning friction factor vs. Reynolds number.

Since friction factor is proportional to $(h/d)^{0.91}$ and to $(p/d)^{-0.54}$, the severity index $\phi = h^2/pd$ can be used as the only parameter that characterises tube roughness' influence on friction factor. The following *general equation* is finally proposed

$$f_a = 1.53(\phi)^{0.46} Re^{-0.16}. \quad (2)$$

Eq. (2) leads to a deviation of 7% for 95% of friction factor experimental data in the region: $Re = 8000$–60 000. In low Reynolds turbulent flow, ($Re = 2000$–8000), the use of Eq. (2) is recommended for tubes with soft corrugation ($\phi < 10^{-3}$); for tubes with a medium-high roughness ($\phi > 10^{-3}$) it is recommended to use a constant friction factor value evaluated with Eq. (2) at $Re = 8000$. If the above-mentioned recommendations are followed, the estimated error stays within ±10%. For Reynolds numbers higher than 60 000 the use of Eq. (2) is still recommended. Consequently, the predicted friction factor values are higher (up to 16%) than the experimental ones (security-side predictions in all cases).

Fig. 7 shows friction factor augmentation produced by corrugated tubes. The increase (f_a/f_s) is determined as the ratio between the experimental friction factor f_a and the smooth tube friction factor f_s, which is calculated by the Blasius equation at the same Reynolds number. Augmentation values between 1.2 and 4 were obtained according mainly to the roughness geometry.

An expression to calculate friction factor augmentation can be obtained as the ratio between Eq. (2) and the Blasius equation

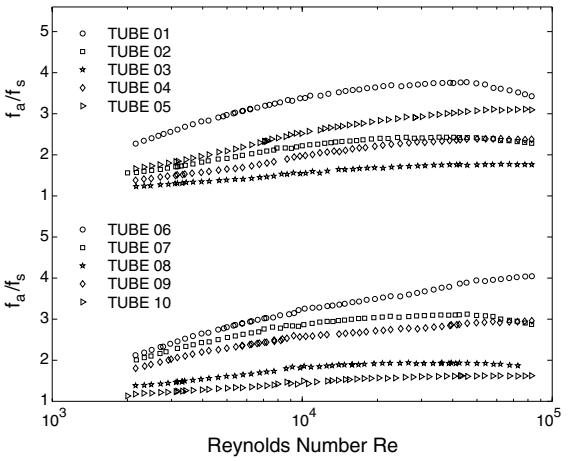

Fig. 7. Friction factor augmentation (f_a/f_s) vs. Reynolds number.

$$f_a/f_s = 19.4(\phi)^{0.46} Re^{0.09}. \quad (3)$$

Eq. (3) shows that pressure drop augmentation depends mainly on severity index $\phi = h^2/pd$ with a slight dependence on Re.

4.1.1. Momentum roughness function $R(h^+)$

Friction factor results were also analysed by using the similarity friction law for roughness surfaces. This analytical model was developed by Nikuradse [15] for sand-grained tubes and used successfully by Webb et al. [16] for correlation pressure drop results for artificial roughness surfaces. Later, some authors as Whiters [4], Sethumadhavan and Raja Rao [7], Mehta and Raja Rao [2] or Zimparov et al. [8], have used this method in order to correlate their experimental results on corrugated tubes.

The roughness function $R(h^+)$ is defined by

$$R(h^+) = \sqrt{2/f_a} + 2.5\ln(2h/d) + 3.75, \quad (4)$$

where h^+ is the roughness Reynolds number ($h^+ = (h/d)Re\sqrt{f_a/2}$).

Experimental pressure drop results are presented in terms of $R(h^+)$ vs. h^+ in Fig. 8. An influence of roughness geometry on $R(h^+)$ is clearly observed: $R(h^+) = \phi(h/d, p/d, h^+)$. This was also found by Webb et al. [16] for transversal ribbed tubes and by Sethumadhavan and Raja Rao [7], Mehta and Raja Rao [2] and Zimparov et al. [8] for corrugated tubes.

It is observed a constant value of $R(h^+)$ at low h^+. At high h^+ the value increases. The following equations in two regions are proposed to correlate $R(h^+)$

$$\begin{aligned} R(h^+) &= 2.60(p/h)^{0.35} && h^+ < 925(p/h)^{-1} \\ R(h^+) &= 1.07(p/h)^{0.48}(h^+)^{0.13} && h^+ > 925(p/h)^{-1} \end{aligned} \quad (5)$$

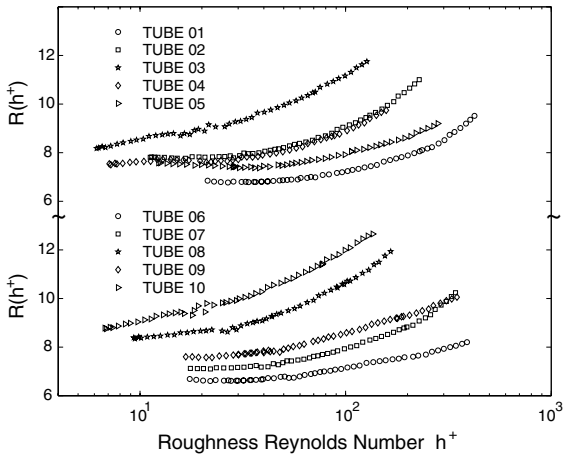

Fig. 8. Momentum roughness function $R(h^+)$ vs. roughness Reynolds number h^+.

Eq. (5) predicts $R(h^+)$ data for corrugated tubes of severity index $\phi > 10^{-3}$ and roughness Reynolds numbers $h^+ = 10$–600 within a standard deviation of 6%. This error in $R(h^+)$ produces a ±8% deviation for the friction factor prediction.

In Fig. 8 it is observed how tubes with high-medium roughness behave qualitatively in a different way to soft roughened tubes 03, 08 and 10 ($\phi < 10^{-3}$). As it will be discussed later, these geometries lack of practical interest, and they have not been taken into account when determining $R(h^+)$ correlation.

4.1.2. Results discussion

Pressure drop experimental results were processed to develop empirical functions for f and $R(h^+)$. These correlations allow a direct comparison with data provided by other experimental works published.

Fig. 6 and Eq. (2) indicate that friction factor decreases with Reynolds number. No asymptotical behaviour has been observed, even in tubes with marked roughness. Experimental results from Ganeshan and Raja Rao [6], Sethumadhavan and Raja Rao [7] and Zimparov et al. [8] reported that friction factor decreases with Reynolds number; an asymptotical behaviour of friction factor with *Re* number is only observed in tubes with a high severity index ($\phi > 5 \times 10^{-3}$). For tubes with severity index values similar to those of this work, *Re* number influence on friction factor can be written as $f \propto Re^{-a}$, where a stays within 0.10 and 0.16 for all cases. Friction factor augmentation given by Eq. (3) has been solved for a corrugated tube of roughness: $h/d = 0.03$ and $p/d = 0.4$, at Reynolds numbers from 5000 to 100 000 and results agree with Zimparov et al. [8] (Fig. 2).

Ravigururajan and Bergles [9] pointed out that whenever corrugated tubes were studied, care should be taken if "sand grain" roughness analytical methods were to be used. The helix angle tends to promote rotation in the main flow. Li et al. [5] determined from flow visualisation by hydrogen bubbles that both longitudinal and spiral flows appear. Deep corrugations with large spiral angles produce swirl flow while in corrugations with spiral angles approaching 90°, the flow pass transversally through the corrugations.

Despite the great amount of published works on corrugated tubes, it can be stated that flow nature has not been yet enough understood. It seems reasonable to consider that two different flows exist: (1) rotation flow and (2) axial flow. Flow rotation depends on helix angle (related to p/d) and how it spreads to main flow depends on flow conditions, namely *Re* number. Axial flow through corrugations may present separations depending on the helical ridge shape and Reynolds number. In transverse rectangular ribs, flow separation exists and its re-attachment depends on p/h relation [16,17]. Plastical deformation does not produce edging shapes and the existence of flow separations cannot be predicted.

Although the flow mechanism is quite complex, friction factor results have been properly correlated in simple mathematical functions. As corrugated tubes of this work present closed helical angles $\alpha = \text{atan}(\pi d/p) = 68$–80°, it is reasonable to assume that flow develops mainly on the axial direction.

On the other hand, experimental results show that the friction factor does not present an asymptotical trend with Reynolds number, as "sand grain" roughened tubes would do. The momentum roughness function $R(h^+)$ was developed from a similarity analysis of "sand grain" roughness. Therefore it may not correlate the pressure drop results better than a friction factor correlation does. In fact the use of $R(h^+)$ function has not improved the fitting of the experimental data in the present work.

It can be stated that pressure drop augmentation in corrugated tubes is produced by: (1) drag forces exerted on the flow field by the ridge, (2) flow blockage due to area reduction, (3) turbulence augmentation and (4) rotational flow produced by the spiral ridge. The flow is highly complex, with a rotational velocity component and possible flow separations, which depends on corrugation geometry and Reynolds number. Hence the correlation of the pressure drop results in corrugated has been more difficult than in dimpled ones (made by the authors [11]) where the flow is more simple.

4.2. Heat transfer

Heat transfer studies under constant heat flux conditions were carried out for both the smooth and the 10 corrugated tubes. A wide flow range was achieved by using two test fluids at different temperatures:

- Water at 40 and 65 °C: Prandtl numbers 4.1 and 2.9 and Reynolds numbers from 3000 to 90 000.
- Ethylene glycol at 40, 55 and 70 °C: Prandtl numbers 92, 59 and 37 and Reynolds numbers from 1500 to 12 000.

Nusselt numbers were determined from measurements on a section located at $x/d = 35$. As the entry region under turbulent flow is very small ($x/d \approx 15$), this local Nusselt number is thus the asymptotic Nusselt number.

Heat transfer tests in a smooth tube were carried out to verify the experimental set-up and the uncertainties analysis. Fig. 9 shows Nusselt number results in comparison to Gnielinski [18] equation,

$$Nu_s = \frac{(f_s/2)(Re - 1000)Pr}{1 + 12.7\sqrt{f_s/2}(Pr^{2/3} - 1)}. \quad (6)$$

Nusselt number results are higher than those predicted by Eq. (6) within a range from 4% to 10%. They have been correlated within a deviation of 3% by the following equation:

$$Nu_s = 0.0344(Re - 1500)^{0.78}Pr^{0.37}. \quad (7)$$

Eq. (7) will be used to determine the heat transfer augmentation produced by corrugated tubes.

Turbulent flow heat transfer experiments were carried out for the corrugated tubes described in Table 2. Eighty experimental points were taken approximately for each tube in order to determine Re and Pr influence on Nu_a. Fig. 10 illustrates the heat transfer augmentation produced by Tube 03 with respect to the smooth tube. The figure shows Nu_a measurements vs. Reynolds for the different Prandtl numbers and it is a sample of the experiments carried out in all tubes.

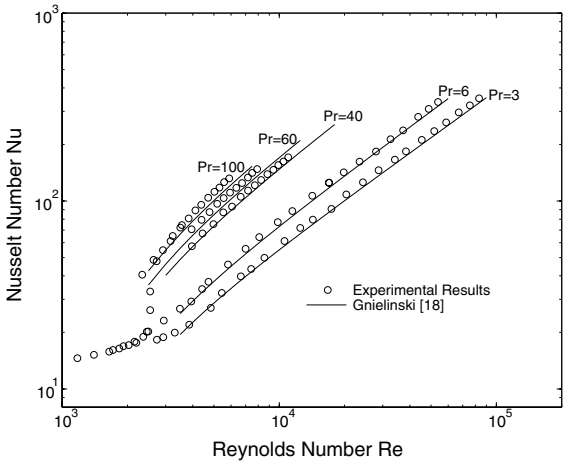

Fig. 9. Nusselt number vs. Reynolds number (smooth tube).

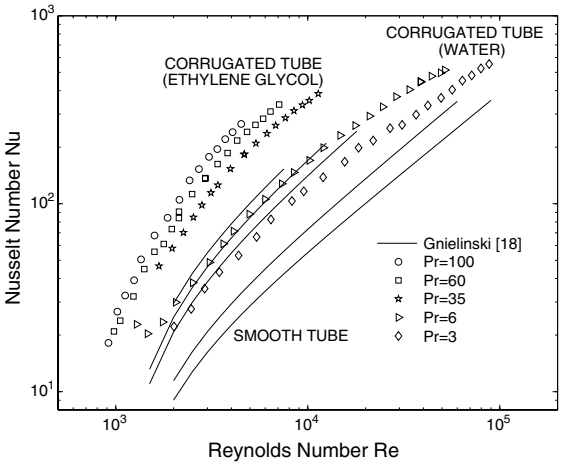

Fig. 10. Nusselt number vs. Reynolds number (Tube 03).

Assuming that corrugated tubes are geometrically similar, it can be stated that a Nusselt number equation in the form $Nu_a = Nu_a(Re, Pr, h/d, p/d)$ can be developed to characterise the tube family. The following correlation was obtained via curve-fitting of heat transfer results for the 10 corrugated tubes (≈800 points):

$$Nu_a = 0.403(h/d)^{0.53}(p/d)^{-0.29}(Re - 1500)^{0.74}Pr^{0.44}. \quad (8)$$

Corrugation pitch and height influence on heat transfer is $Nu_a \propto (h/d)^{0.53}(p/d)^{-0.29}$. This shows severity index ($\phi = h^2/pd$) to be the unique geometric parameter to characterise heat transfer augmentation produced by corrugated tubes. The following *general equation* correlates 95% of experimental data within a deviation of 14%

$$Nu_a = 0.374(\phi)^{0.25}(Re - 1500)^{0.74}Pr^{0.44}. \quad (9)$$

Eq. (9) shows that Prandtl number's influence on heat transfer is $Nu_a \propto Pr^{0.44}$. The exponent for the smooth tube is Pr is 0.37. Therefore it can be concluded that the heat transfer augmentation produced by corrugated tubes increases with Prandtl number. The Nusselt number augmentation can be evaluated as the ratio between Nu_a (Eq. (9)) and Nu_s (Eq. (7)), resulting

$$Nu_a/Nu_s = 10.9(\phi)^{0.25}(Re - 1500)^{-0.04}Pr^{0.07}. \quad (10)$$

As an example, Fig. 11 shows Nusselt number augmentation Nu_a/Nu_s for Tubes 01, 02 and 03 at Prandtl numbers 6 and 60.

4.2.1. Heat transfer roughness function $G(h^+)$

Heat transfer results were also analysed in terms of the heat transfer roughness function $G(h^+, Pr)$, developed by Dipprey and Sabersky [19]. This function was first used by Webb et al. [16] and later by many other authors to analyse their experimental data from artificial

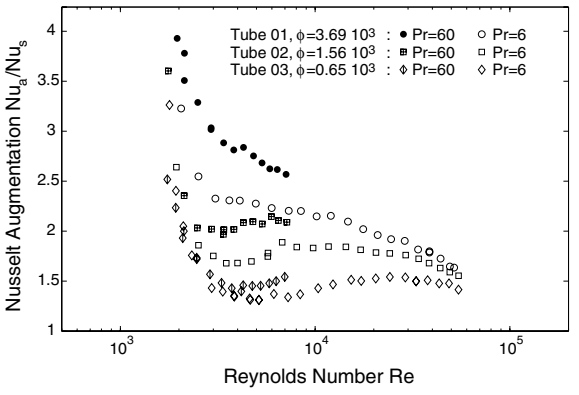

Fig. 11. Nusselt number augmentation (Nu_a/Nu_s) for Tubes 01, 02 and 03 at Prandtl numbers 6 and 60.

roughness surfaces. The heat transfer roughness function can be written as the product of $G(h^+)Pr^n$

$$G(h^+)Pr^n = \frac{f_a/(2St) - 1}{\sqrt{f_a/2}} + R(h^+). \tag{11}$$

The experimental results have been processed in this way and the dependence on Prandtl number was found to be $G(h^+) \propto Pr^{0.57}$.

Fig. 12 shows $G(h^+)Pr^{-0.57}$ as a function of roughness Reynolds number h^+. Two different regions are observed depending on h^+ range. The following equations are proposed

$$\begin{aligned} G(h^+)Pr^{-0.57} &= 14.3 && h^+ = 15\text{–}60 \\ G(h^+)Pr^{-0.57} &= 5.13(h^+)^{0.25} && h^+ = 60\text{–}600 \end{aligned} \tag{12}$$

These equations along with Eq. (12) for $R(h^+)$ leads to a deviation in the calculated Nusselt number within ±12.5% in the h^+ range from 15 to 600.

4.2.2. Results discussion

The present paper presents a large amount of experimental data covering a wide Prandtl number range. This is indeed the main contribution of the work as it allows to establish the Prandtl number influence on heat transfer with good precision. Webb [20] indicated that Prandtl number dependence was an unsettled problem since there are few experimental studies that have studied this subject so far. The only works which can be taken as reference studies are those from Webb et al. [16] and Sethumadhavan and Raja Rao [7].

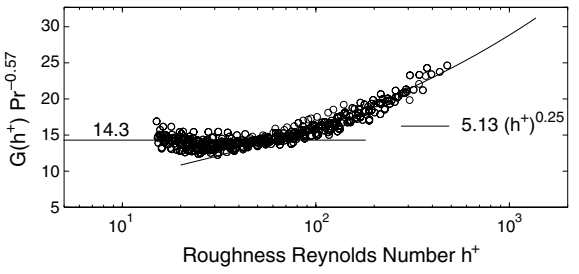

Fig. 12. Heat transfer roughness function $G(h^+)Pr^{-0.57}$ vs. roughness Reynolds number h^+.

The analysis of Eq. (10) shows that Nusselt number augmentation produced by corrugated tubes depends on: (1) roughness geometry (quantified by the severity index ϕ), (2) flow conditions (Re number) and (3) physical fluid properties (Pr number). Nusselt number augmentation given by Eq. (10) has been solved for a corrugated tube of roughness: $h/d = 0.03$ and $p/d = 0.4$, at flow conditions $Pr = 6$ and $Re = 5000$–$100\,000$ and results agree with Li et al. [5] (Fig. 3).

As it was expected, tubes with the highest severity index present the highest heat transfer augmentation. Experimental results show that Nusselt number augmentation (Nu_a/Nu_s) increases with Prandtl number and decreases with Reynolds number. Heat transfer increases up to 200% ($Nu_a/Nu_s \approx 3$) can be obtained for Reynolds numbers lower than 5000 and at Prandtl number 60. On the other hand, at $Re = 90\,000$ and $Pr = 2.5$ the maximum heat transfer augmentation is $Nu_a/Nu_s \approx 1.75$.

This behaviour can be explained because for turbulent flows the dominant thermal resistance is concentrated at a thin boundary layer. Its thickness depends on Reynolds and Prandtl numbers. A wide thermal boundary layer is expected at low Reynolds numbers and at high Prandtl numbers. These are the conditions where the mixing of the flow produced by corrugation is more effective.

Heat transfer results have been presented by the heat transfer roughness function $G(h^+, Pr)$. The result obtained, $G(h^+) \propto Pr^{0.57}$, agrees with the one reported by Webb et al. [16], and it is slightly different from the one reported by Sethumadhavan and Raja Rao [7] ($G(h^+) \propto Pr^{0.55}$).

5. Performance evaluation, roughness optimisation

Bergles et al. [21] and Webb [22] proposed several performance criteria to evaluate the thermohydraulic performance of enhanced tubes. In this paper, only the criterion $R3$ outlined by Bergles et al. [21] is calculated to quantify the benefits from corrugated tubes. The criterion is defined by $R3 = Nu_a/Nu_o$ where Nu_a is the heat transfer obtained with the corrugated tube and Nu_o is the heat transfer obtained with an smooth tube for equal pumping power and heat exchange surface area. To satisfy the constrain of equal pumping power, Nu_o is evaluated at the equivalent smooth tube Reynolds number Re_o, which matches

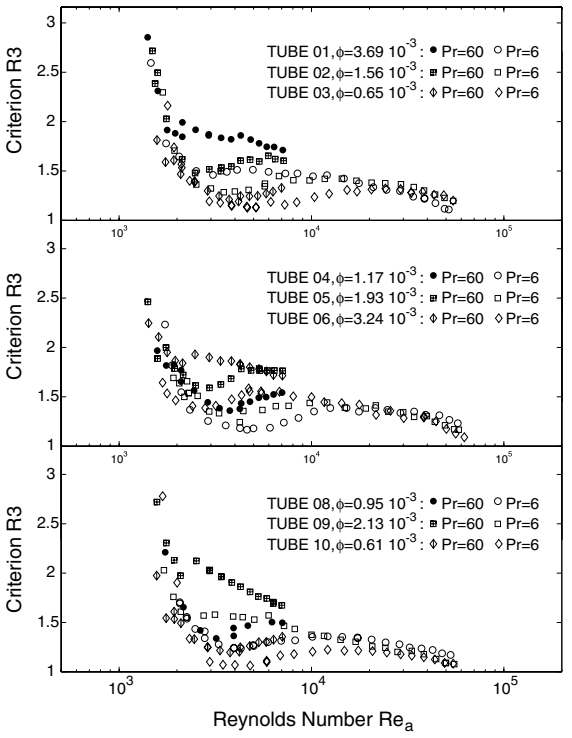

Fig. 13. Performance evaluation criterion $R3$ vs. Re for Prandtl numbers 6 and 60.

$$f_a Re_a^3 = f_o Re_o^3. \tag{13}$$

Fig. 13 shows the performance parameter $R3$ for the corrugated tube family at Prandtl numbers 6 and 60. As it was expected, it is observed that the performance improves with Prandtl number.

At low Reynolds numbers ($Re < 10\,000$), tubes with the best performance are the ones with the highest severity index ($\phi > 3 \times 10^{-3}$). Heat transfer enhancements around 100% ($R3 = 2$) at $Pr = 60$ and around 50% ($R3 = 1.5$) at $Pr = 6$ are obtained when smooth tubes are directly replaced by corrugated ones.

On the other hand, at high Reynolds numbers ($Re = 10\,000$–$40\,000$), tubes with intermediate roughness ($\phi = 1$–2×10^{-3}) are more suitable. At these Reynolds numbers, enhancements around 50% ($R3 = 1.5$) can be obtained. The analysis allows to state that low roughened tubes ($\phi < 10^{-3}$) are not advantageous in practical applications.

Results show that the selection of a corrugated tube for a particular application depends on flow conditions. Fig. 14 shows the performance evaluation criterion $R3$ vs. the severity index ϕ, for Prandtl numbers 6 and 60 and different Reynolds numbers. The figure shows that for low Reynolds numbers the best choice is to select high-roughened tubes (like Tube 01). However at higher Reynolds numbers, the most appropriate is to employ

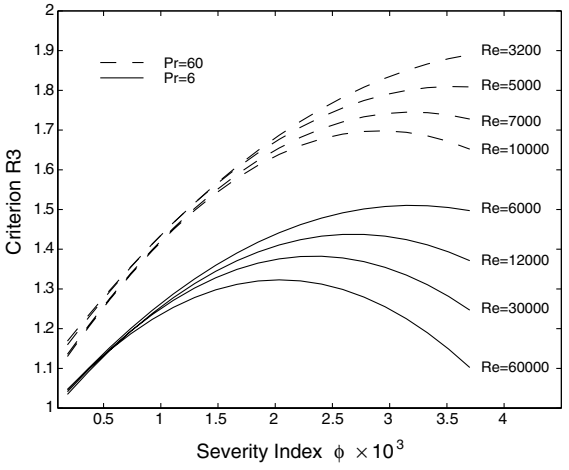

Fig. 14. Roughness optimisation following $R3$ (proposed by Bergles et al. [21]).

corrugated tubes with severity index around 1.5 to 2×10^{-3} (Tubes 02 or 05).

6. Conclusions

(1) A comprehensive experimental study has been carried out on a family of corrugated tubes. Corrugated tubes present higher-pressure drop and heat transfer than the smooth tube under the same flow conditions. Increases from 20% to 300% in friction factor coefficient and up to 250% in Nusselt number were observed.

(2) General correlations were drawn so as to characterise the studied corrugated tubes family. The severity index ($\phi = h^2/pd$) has been employed as the unique geometric parameter to characterise roughness influence on flow.

(3) Measurements were taken at five different Prandtl numbers in order to establish accurately Prandtl influence on heat transfer, which was found to be $Nu_a \propto Pr^{0.44}$. Therefore, heat transfer augmentation produced by corrugated tubes increases with Prandtl number.

(4) According to the performance evaluation criterion $R3$ suggested by Bergles et al. [21], an optimisation analysis was carried out. At low Reynolds numbers ($Re < 10\,000$), the most advantageous tubes are those with the highest severity index ($\phi > 3 \times 10^{-3}$) while at high Reynolds numbers ($Re = 10\,000$–$40\,000$), the best choice is to employ tubes with intermediate roughness ($\phi = 1$–2×10^{-3}).

(5) The present study broadens considerably the experimental data carried out on corrugated tubes at Prandtl numbers higher than typical water values. Corrugated tubes with similar geometry to those studied in the current work have been characterised. Correlations

obtained from pressure drop and heat transfer experiments can be employed for design purposes with a high level of accuracy and under a wide range of flow conditions: $Re = 2000$–$90\,000$ and $Pr = 2.5$–100.

Acknowledgements

This research has been partially financed over the 1FD1997-0211 (TYP) grant of the ''Dirección General de Enseñanza Superior e Investigación Científica'' in Spain and the HRS Spiratube company from Murcia (Spain).

References

[1] T.J. Rabas, A.E. Bergles, D.L. Moen, Heat transfer and pressure drop correlations for spirally grooved (rope) tubes used in surface condensers and multistage flash evaporators, in: Augmentation of Heat Transfer in Energy Systems, ASME Symposium, HTD-Vol 52, ASME, New York, 1988, pp. 693–704.

[2] M.H. Mehta, M. Raja Rao, Investigations on heat transfer and frictional characteristic of enhanced tubes for condensers, in: Advances in Enhanced Heat Transfer, ASME, New York, 1979, pp. 11–21.

[3] R.K. Gupta, M. Raja Rao, Heat transfer and friction characteristics of Newtonian and power law type of non Newtonian fluids in smooth and spirally corrugated tubes, in: Advances in Enhanced Heat Transfer, ASME, New York, 1979, pp. 103–113.

[4] J.G. Withers, Tubeside heat transfer and pressure drop for tubes having helical internal ridging with turbulent/transitional flow of single phase fluid. part I-single-helix ridging, Heat Transfer Eng. J. 1 (1980) 48–58.

[5] H.M. Li, K.S. Ye, Y.K. Tan, S.J. Deng, Investigation of tube-side flow visualisation. Friction factor and heat transfer characteristics of helical-ridging tubes, in: Proceedings of the 7th Heat Transfer Conference, Hemisphere Publishing Corp., Washington, 1998, pp. 75–80.

[6] S. Ganeshan, M. Raja Rao, Studies on thermohydraulics of single and multistart spirally corrugated tubes for water and time-dependent power law fluids, Int. J. Heat Mass Transfer 25 (1982) 1013–1022.

[7] R. Sethumadhavan, M. Raja Rao, Turbulent flow friction and heat transfer characteristics of single and multistart spirally enhanced tubes, J. Heat Transfer 108 (1986) 55–61.

[8] V.D. Zimparov, N.L. Vulchanov, L.B. Delov, Heat transfer and friction characteristics of spirally corrugated tubes for power plant condensers—1. Experimental investigation and performance evaluation, Int. J. Heat Mass Transfer 34 (1991) 2187–2197.

[9] T.S. Ravigururajan, A.E. Bergles, Prandtl number influence on heat transfer enhancement in turbulent flow of water at low temperatures, Trans. ASME 117 (1995) 276–282.

[10] W.J. Marner, A.E. Bergles, J.M. Chenoweth, On the presentation of performance data for enhanced tubes used in shell-and-tube heat exchangers, J. Heat Transfer 105 (1983) 358–365.

[11] P.G. Vicente, A. Garcia, A. Viedma, Heat transfer and pressure drop for low Reynolds turbulent flow in helically dimpled tubes, Int. J. Heat Mass Transfer 45 (2002) 543–553.

[12] P.G. Vicente, Te cnicas de mejora de la transferencia de calor en tubos para intercambiadores de calor industriales en flujo monofa sico laminar y turbulento, Tesis doctoral, 2002.

[13] W.M. Kays, A.L. London, Compact Heat Exchangers, third ed., McGraw-Hill, New York, 1984.

[14] S.J. Kline, F.A. McClintock, Describing uncertainties in single sample experiments, Mech. Eng. 75 (1953) 3–8.

[15] J. Nikuradse, Laws of flow in rough pipes, VDI Forschungsheft, 1933, p. 361, English translation, NACA TM-1292, 1965.

[16] R.L. Webb, R.G. Eckert, R.J. Goldstein, Heat transfer and friction in tubes with repeated-rib roughness, Int. J. Heat Mass Transfer 14 (1971) 601–617.

[17] B. Arman, T.J. Rabas, Influence of rib width on the performance of enhanced tubes with the separation and reattachment mechanism, in: Fundamentals of Forced Convection Heat Transfer, ASME HTD 210, 1992, pp. 159–166.

[18] V. Gnielinski, New equations for heat and mass transfer in turbulent pipe and channel flow, Int. Chem. Eng. 16 (1976) 359–368.

[19] D.F. Dipprey, R.H. Sabersky, Heat and momentum transfer in smooth and rough tubes at various Prandtl numbers, Int. J. Heat Mass Transfer 6 (1963) 329–353.

[20] R.L. Webb, Principles of Enhanced Heat Transfer, first ed., Wiley Interscience, New York, 1994, pp. 229–284.

[21] A.E. Bergles, A.R. Blumenkrantz, J. Taborek, Performance evaluation criteria for enhanced heat transfer surfaces, J. Heat Transfer 2 (1974) 239–243.

[22] R.L. Webb, Performance evaluation criteria for use of enhanced heat transfer surfaces in heat exchanger design, Int. J. Heat Mass Transfer 24 (1981) 715–726.